Low-temperature synthesis of nanoscale silica multilayers – atomic layer deposition in a test tube

Benjamin Hatton,*[a] Vladimir Kitaev,[b] Doug Perovic,[c] Geoff Ozin[d] and Joanna Aizenberg[a]

Received 14th March 2010, Accepted 29th April 2010
DOI: 10.1039/c0jm00696c

Herein we demonstrate a simplified, '*poor-man's*' form of the Atomic Layer Deposition (ALD) technique to grow uniform silica multilayers onto hydrophilic surfaces at low temperatures, including room temperature (RT). Tetramethoxysilane vapor is used alternately with ammonia vapor as a catalyst, with very common benchtop lab equipment in an ambient environment. This deposition method could be applied in a wide range of fields for growing nanoscale layers of silica from an inexpensive vapor source, without the sophisticated vacuum systems or high temperatures that are generally required for ALD. Conditions for uniform deposition are demonstrated for 20-nm-thick silica shells grown around polymer spheres at RT, and in the interstitial space of a colloidal crystal film. This approach is shown to provide a controlled means of sintering the silica spheres and thereby is an easy way to modify the photonic and mechanical properties of the resulting material. We believe this method has an advantage compared to other more sophisticated methods of ALD and provides a simple technique for broad applications in MEMs, nanoporous structures, sintering of components, cell encapsulation, and organic/inorganic layered composites.

Introduction

Amorphous silica (SiO_2) is a widespread and versatile material for a diverse range of nano- and microscale applications, and it is found in a vast variety of natural and technological structures, ranging from diatom shells and sea sponge skeletons,[1] to MEMS structural components,[2] and microelectronic dielectric layers.[3] The rotational freedom of the siloxane (Si–O–Si) bond between $[SiO_4]^{4-}$ tetrahedra allows silica to adopt a variety of stable 3D geometries for nanoscale structures as small as 1-2 nm.[4] Furthermore, optical and chemical properties of the resulting material can be tuned through surface functionalization,[5,6] or conversion to materials such as TiO_2 or Si through exchange reactions.[7,8]

Deposition of silica can be achieved from the vapor phase by chemical vapor deposition (CVD), sputtering or atomic layer deposition (ALD). ALD is a technique for growing monolayers of materials using self-limiting surface reactions with reactive vapor precursors, and sequentially depositing such monolayers into a film of controlled thickness.[9–11] A wide range of inorganic materials, including Al_2O_3, TiO_2, ZnO, and ZnS can be grown as uniform layers of highly-controlled thickness 0.10∼0.20 nm per step. However, the high temperatures (*i.e.*; 150 to 500 °C) and vacuum conditions that are normally required can limit ALD for widespread use. Therefore, techniques for the controlled deposition of metal oxides at lower temperatures are useful for coating material without distorting the underlying structure, which is particularly necessary for inorganic deposition on organic and biological surfaces or templates. For example, Yu *et al.*[12] recently demonstrated a 3D nanolithography method based on the conformal coating of Al_2O_3 ALD inorganic layers on polymer spheres at 80 °C.

Room temperature (RT) ALD synthesis of silica can be achieved with $SiCl_4$ vapor through reaction with surface hydroxyl groups (in the presence of NH_3 catalyst), hydrolysis of the remaining Si–Cl bonds by H_2O, and condensation polymerization to create a new silica layer.[13,14] These two reactions can be alternated to grow multilayers of uniform and controlled thickness, at a rate of 0.20 nm per cycle. Previous applications of $SiCl_4$ ALD at RT have been for sintering silica spheres in a colloidal crystal,[15] and for silica ribbons grown along a graphite step edge.[16] However, $SiCl_4$ is highly moisture-sensitive and it generates a HCl byproduct, which bring significant practical disadvantages.

Ferguson *et al.*[17] demonstrated by FTIR spectroscopy that tetraethoxysilane (TEOS) could be used for SiO_2 ALD at RT, using NH_3 as a catalyst. Other examples of silica layer growth at low temperatures using TEOS vapor, include the infiltrated growth in a surfactant template (at 90 °C),[18] an encapsulation layer around biological cells (at RT),[19] and the structural enhancement of a mesoporous silica film (at 130 °C).[20] However, none of these examples include the controlled growth by sequential multilayers. Herein, we demonstrate the application of alkoxysilane vapor (tetramethoxysilane, TMOS) for the low-temperature growth of multiple silica layers, using inexpensive benchtop lab equipment and in an ambient environment. We illustrate this TMOS ALD method by growing silica multilayers around polymer colloidal spheres and within a colloidal crystal (opal) structure. The rapid and simple nature of this method means it could easily be applied in any physics, chemistry or

[a]*School of Engineering and Applied Sciences, Wyss Institute for Biologically Inspired Engineering, Harvard University, Cambridge, MA, USA. E-mail: bhatton@seas.harvard.edu; jaizenberg@seas.harvard.edu*
[b]*Dept of Chemistry, Wilfrid Laurier University, Waterloo, Ontario, Canada*
[c]*Dept of Materials Science and Engineering, University of Toronto, Toronto, Ontario, Canada*
[d]*Dept of Chemistry, University of Toronto, Toronto, Ontario, Canada*

This journal is © The Royal Society of Chemistry 2010

biology lab for the controlled deposition of nanoscale silica layers without the need for a sophisticated ALD system.

Experimental

The silica growth was performed in a fumehood, using two 25 mL glass test tubes (1 cm diameter) containing ~ 5 mL of TMOS (Sigma-Aldrich, 98%) and ~ 5 mL ammonium hydroxide (Sigma-Aldrich, 30 Wt% solution), respectively (Fig. 1). Substrate samples were attached to a metal wire and suspended alternately in each of the test tubes, approximately 2 cm above the liquid surface, for periods of time discussed below. As a result, the substrate samples were exposed sequentially to TMOS and NH_3/H_2O vapors.

Two experimental conditions were tested for silica growth. The first involved SiO_2 deposition onto SiO_2 colloidal crystal (opal) films at 80 °C. Films were prepared using two batches of mono-dispersed SiO_2 spheres (approximately 5% size variation) of average diameters 285 nm and 320 nm, synthesized by a modified Stöber method,[21] and deposited onto glass slides (precleaned with Piranha solution) by evaporative self-assembly[22] using 1 vol% suspensions in ethanol. Substrate samples were alternated between the TMOS test tube (partially immersed in an 80 °C oil bath) and the NH_4OH test tube (at RT) for 60 s and 10 min, respectively. Every 10 exposure cycles the films were exposed to oxygen plasma for 10 min (Technics Micro RIE 800, 200W), to help ensure sufficient surface hydroxylation.

Scanning electron microscopy (SEM) was performed using a Hitachi S-4500 at 1 kV (no Au coating), a JEOL 5600 (20 kV, with sputtered Au), or a Zeiss Ultra (10 kV, with sputtered Au). A transmission electron microscope (TEM) (JEOL 2100) was used at 200 kV to image the SiO_2 shells deposited onto a carbon-coated Cu grid. Optical measurements were made in reflectance using an Ocean Optics fiber optic UV-Vis spectrometer (SD-20) integrated through the eyepiece with an optical microscope (Olympus BX-51), using a 20X objective.

The Young's modulus (E) and hardness (H) of the films were measured using nanoindentation (Shimadzu DUH-2100) with a Berkovich 3-sided diamond indenter at loads from 0.1 to 10 mN. For each measurement, 4 load/unload cycles were used with a 60 s ramp and a 5 s holding time, and then analyzed using the Oliver/Pharr procedure,[23] assuming a Poisson ratio of 0.20.

Fig. 1 Experimental setup for the exposure of samples to $Si(OCH_3)_4$ (TMOS) and NH_3 vapor, using $NH_3 \cdot H_2O$ solution. Samples were suspended from a wire within each of the two 25 mL test tubes.

The second experiment involved room temperature (RT) deposition onto 450 nm diameter polystyrene (PS) spheres (Invitrogen, sulfate-terminated) to produce SiO_2 shells. The spheres were immobilized onto a clean Si wafer substrate by drying a 100 μL volume of 2% aqueous suspension, and exposed to 5 cycles of 10 min and 20 min in the TMOS and NH_4OH test tubes at RT, respectively. The Si substrate was then heated at 450 °C for 2 h (in air, 5 h ramp) to burn away the polymer sphere template.

Results and discussion

The growth of nanoscale silica multilayers was performed in a simple experimental setup shown in Fig. 1, by alternating the exposure of the substrate samples to TMOS and NH_3/H_2O vapors. The NH_3 vapor catalyzes the hydrolysis of remaining methoxy groups and aids the condensation polymerization of surface silanol groups.

TMOS-based SiO_2 growth at 80 °C was used to gradually fill the interstitial space of a SiO_2 colloidal crystal film. Fig. 2 presents SEM images of the 320 nm opal film with increasing TMOS exposure cycles from 0 to 100, showing an increasing, uniform growth of silica multilayers in the interstitial space, through the thickness of the film. The growth of necks between spheres begins at the contact points, as apparent in the image corresponding to 40 cycles. After ~100 exposure cycles the available interstitial space is almost completely infiltrated with silica throughout the film, to the point at which the residual interstitial volume likely remains unfilled due to blockage of the interconnected pores.

Controlling the pore size and lattice connectivity of colloidal crystals has an important influence on their available surface area and optical, mechanical and fluid transport properties. The 'necking' of colloidal spheres can be controlled by thermal sintering (*i.e.*; 700–1100 °C for silica), but this also causes a contraction of the center-to-center distance between particles, to cause distortion and cracking.[24] Therefore, simple techniques to grow layers around the spheres without distorting the opal structure are very useful to control the porosity and increase the mechanical stability.[15] While conventional CVD and ALD vapor phase growth on colloidal crystals has been demonstrated previously,[25–28] our results demonstrate that low-temperature TMOS-ALD is a simple method to control SiO_2 layer growth. To demonstrate the applicability of our method to tune these macroscopically measured properties, the changes in optical and mechanical properties were characterized as a function of silica deposition cycles. A simple means to estimate the infiltration growth within an opal is from the position of the first stop gap (λ_{111}) in an optical spectrum (corresponding to the (111) plane), given by,[29]

$$\lambda_{(111)} = 2 \cdot d_{(111)} \cdot \sqrt{\langle \varepsilon \rangle - \sin^2\theta} \quad (1)$$

where $d_{(111)}$ is the interplanar distance of the (111) planes, θ is the incidence angle, and ⟨ε⟩ is the volume-averaged dielectric constant of the air/solid composite structure. Fig. 3a shows the

This journal is © The Royal Society of Chemistry 2010

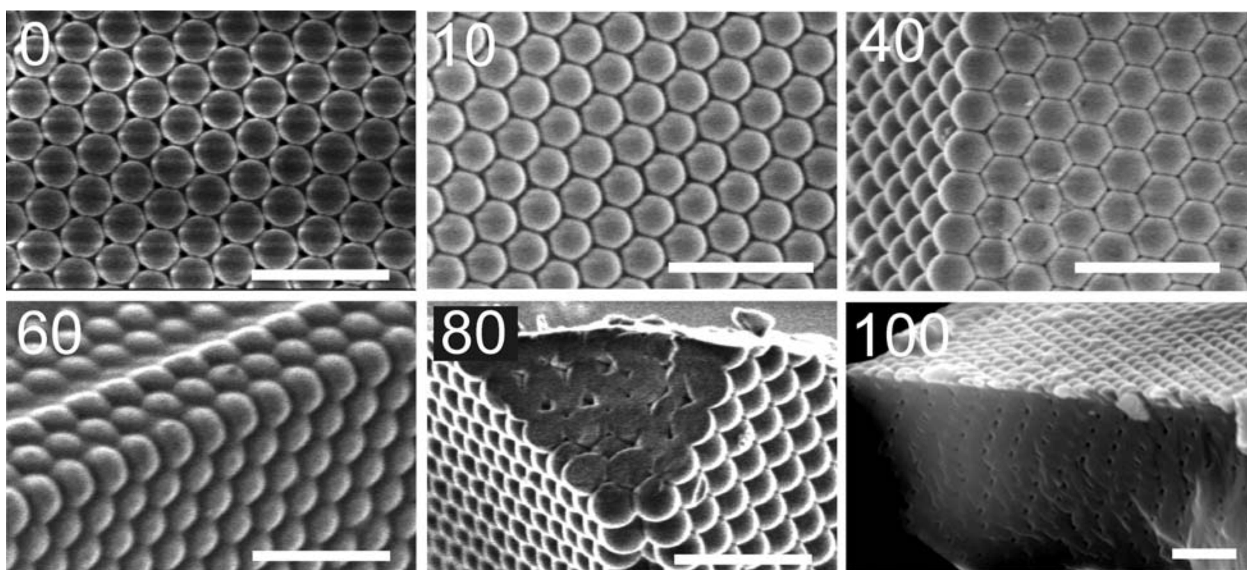

Fig. 2 SEM images of the opal film composed of the 320 nm SiO_2 colloids after increasing interstitial SiO_2 deposition, where the number of TMOS exposure cycles is indicated (scale bar = 1 μm).

optical spectra for the 320 nm opal film as a function of the number of the TMOS exposure cycles (from 0 to 100), indicating the red-shift (*i.e.*; increase in the effective refractive index, n_{eff}) and reduced intensity of the λ_{111} Bragg peak with increased silica deposition. λ_{111} of the films composed of 285 and 320 nm silica colloids increases from 584 to 657 nm (over 104 cycles), and from 670 to 745 nm (100 cycles), respectively. These end points both represent near full infiltration, as indicated by a small plateau in the peak shift. The calculated values for n_{eff} increase from 1.256 to 1.415 and 1.285 to 1.427, for the 285 and 320 nm films, respectively. Accordingly, the silica volume fraction (V_s) shown in Fig. 3b increased to approximately 0.93 and 0.97 for the 285 and 320 nm films, respectively (assuming $n_{SiO2} = 1.44$). If the spheres were fully dense one would expect V_s to start at 0.74 for a close-packed structure (dotted line). Therefore, this simple model suggests there is densification of the silica spheres themselves, in addition to external layer growth between the spheres.

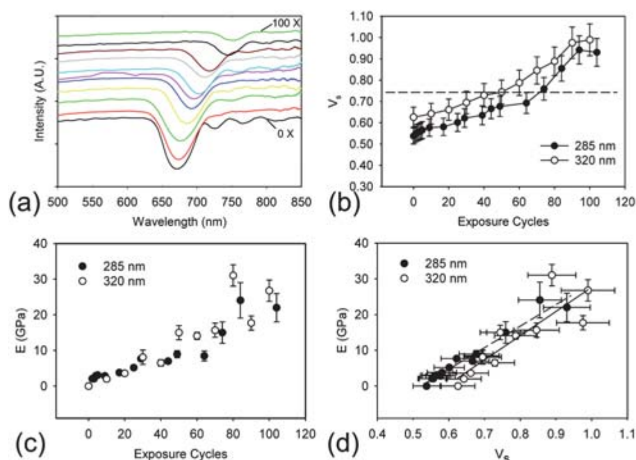

Fig. 3 Characterization of optical and mechanical properties of SiO_2-coated colloidal crystals. (a) absorption optical spectra of the opal film composed of 320 nm SiO_2 colloids after increasing numbers of TMOS exposure cycles, from 0X (bottom) to 100X (top), showing a continuous shift of the {111} Bragg peak; (b) increasing silica volume fraction (V_S), with TMOS exposure cycles, calculated for the 285 and 320 nm opal films; (c) change in the Young's modulus (E) with increasing TMOS exposure cycles; and (d) the relationship between E and V_S, for the 285 and 320 nm opal films.

The results indicate the average deposition rate is between 0.2 - 0.3 nm per TMOS exposure cycle, which is 3 - 4 times increased compared to 0.07 - 0.08 nm per cycle for NH_3-catalyzed TEOS ALD at RT, measured by Ferguson *et al.*[17] This growth rate depends on the relative humidity, and the thickness of the adsorbed hydration layer.[30] While a more sophisticated, closed vacuum system is necessary to control these factors, our results demonstrate that the conditions of the ambient atmosphere are *sufficiently* suitable to achieve reasonable, nanoscale control over the layer thickness.

The mechanical strength of colloidal crystals (composed of a loosely bound aggregate of particles) is typically extremely low. We have characterized the mechanical properties of the colloidal crystal coated with the successive layers of SiO_2. The Young's modulus (E) is shown in Fig. 3c as a function of TMOS exposure cycles. For the 285 nm and 320 nm films, E increases from practically zero to ~ 25 GPa and ~ 30 GPa, respectively, near the points of maximum silica infiltration (dense amorphous silica ~ 70 GPa). A plot of E versus V_s (Fig. 3d) suggests a linear relationship, though the statistical variation is too high to define with certainty. The elasticity of porous solids generally shows a power law behavior with respect to the relative density, but depends on the porosity range, structural symmetry, geometry and connectivity to a great extent.[31,32]

The continuous shift of these optical and mechanical properties values with increasing SiO_2 deposition further demonstrates the uniform distribution of the grown SiO_2 layers in a quantitative fashion (in addition to the qualitative evidence of SEM cross-sections).

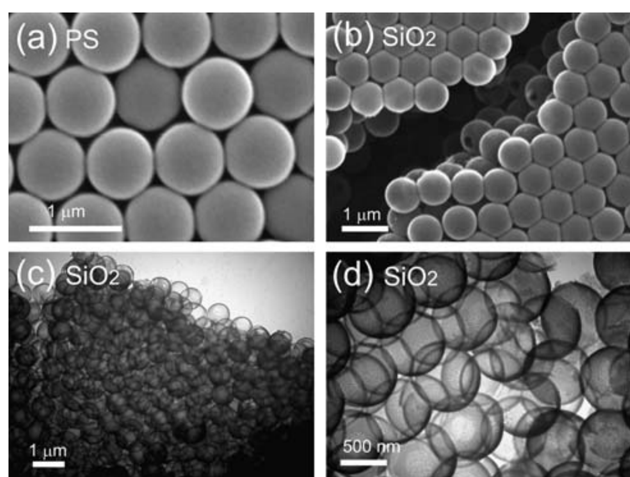

Fig. 4 Room-temperature deposition of SiO_2 on PS spheres. (a) SEM of 700 nm PS spheres before SiO_2 deposition; (b) SEM of SiO_2 shells remaining after 5 growth cycles at RT around the PS sphere template and calcination at 450 °C; (c)-(d) Low- and high-magnification TEM images of the SiO_2 shells from (b), showing highly uniform SiO_2 wall thicknesses around 20 nm thick.

Silica growth was tested at RT conditions, to further increase the versatility of this method towards lower temperatures. Fig. 4 shows RT deposition (5 cycles) was found to uniformly coat the 700 nm PS spheres (Fig. 4a) with a SiO_2 layer around 20 nm thick, as shown in the SEM (Fig. 4b), and TEM (Fig. 4c,d) images of the porous shells that remain after the polymer template decomposition. The SiO_2 layer appears to evenly deposit throughout the structure of spheres, to create a coating with roughness on the order of 2-3 nm, as estimated from TEM imaging. In principle, higher temperatures (*i.e.*; 600–800 °C) could be used to further increase the densification of the SiO_2 shell walls, if needed. These results show that this method of SiO_2 growth at RT is a very easy way to deposit nanoscale SiO_2 structures using common, inexpensive equipment and chemical reagents.

There are many advantages of vapor phase growth over solution-based growth, such as the avoidance of capillary effects. Our method also gets around the high reactivity of $SiCl_4$ as a reagent, which requires a closed (moisture-free) environment. In general, ALD processes have an advantage of involving *self-limiting* surface reactions, as long as adequate care is taken to catalyze the reaction, and maintain a sufficient density of hydroxyl groups to continue. We have demonstrated suitable conditions for TMOS vapor, using NH_3 as a catalyst, in an ambient atmosphere. Thus, even without a sophisticated control over the humidity and H_2O adsorption, we have achieved a quite uniform growth of silica multilayers. Further work shall determine to what extent these ambient conditions can be applied to other alkoxide precursors, depending on their volatility and reactivity. The growth rate of SiO_2 layers on the SiO_2 spheres using the 80 °C conditions was approximately 0.2-0.3 nm per exposure. The growth rate on PS spheres under RT conditions was found to be much faster (4-5 nm/exposure), which may be due to the extended exposure time in TMOS vapor, and/or a reflection of uptake of TMOS vapor into the polymer surface, as an absorptive swelling process.

In conclusion, we have demonstrated a method for the low-temperature deposition of uniform, well-controlled, nanometer-scale silica layers that show high connectivity and mechanical stability by a very basic form of ALD using a simple alkoxide precursor, and inexpensive, benchtop lab equipment. Silica growth under these mild conditions is well-suited to preserving the fine details of the underlying structure or template. Altogether, this benchtop method for silica deposition does not have the same level of control as conventional ALD methods, but we believe it offers an important advantage of being extremely versatile and easy to use in any chemistry, physics or biology lab. There are a wide range of possible applications for nano/micro-scale growth of silica layers that would benefit from the simplicity of this method, such as in the engineering of MEMS structures,[33] the fabrication of high-surface-area, porous shell structures, tuning the porosity of materials such as nanoporous inverse opal film,[34] 3D nanofabrication,[12] sintering of particle-based films,[15] cell encapsulation,[19] and organic/inorganic layered composites.

Acknowledgements

This project was supported by the Office of Naval Research under Award N00014-07-1-0690-DOD35CAP.

References

1 S. Mann, *Biomineralization: principles and concepts in bioinorganic materials chemistry*, Oxford University Press, Oxford, 2001.
2 S. M. Spearing, *Acta Mater.*, 2000, **48**, 179–196.
3 M. J. Madou, *Fundamentals of Microfabrication: The Science of Miniaturization*, CRC Press, 2002.
4 S. L. Gillet, in *Fifth Foresight Conference on Molecular Nanotechnology*, Palo Alto, California, 1997.
5 P. Van Der Voort and E. F. Vansant, *J. Liq. Chromatogr. Relat. Technol.*, 1996, **19**, 2723–2752.
6 M. L. Hair and C. P. Tripp, *Colloids Surf., A*, 1995, **105**, 95–103.
7 Z. Bao, M. R. Weatherspoon, S. Shian, Y. Cai, P. D. Graham, S. M. Allan, G. Ahmad, M. B. Dickerson, B. C. Church, Z. Kang, H. W. Abernathy III, C. J. Summers, M. Liu and K. H. Sandhage, *Nature*, 2007, **446**, 172–175.
8 S.-J. Lee, S. Shian, C.-H. Huang and K. H. Sandhage, *J. Am. Ceram. Soc.*, 2007, **90**, 1632–1636.
9 S. M. George, A. W. Ott and J. W. Klaus, *J. Phys. Chem.*, 1996, **100**, 13121–13131.
10 M. Leskela and M. Ritala, *Thin Solid Films*, 2002, **409**, 138–146.
11 G. Clavel, E. Rauwel, M.-G. Willinger and N. Pinna, *J. Mater. Chem.*, 2009, **19**, 454–462.
12 X. Yu, H. Zhang, J. K. Oliverio and P. V. Braun, *Nano Lett.*, 2009, **9**, 4424–4427.
13 J. W. Klaus, O. Sneh and S. M. George, *Science*, 1997, **278**, 1934–1936.
14 J. W. Klaus and S. M. George, *J. Electrochem. Soc.*, 2000, **147**, 2658–2664.
15 H. Miguez, N. Tetreault, B. D. Hatton, S. M. Yang, D. D. Perovic and G. A. Ozin, *Chem. Commun.*, 2002, 2736–2737.
16 M. P. Zach, J. T. Newberg, L. Sierra, J. C. Hemminger and R. M. Penner, *J. Phys. Chem. B*, 2003, **107**, 5393–5397.
17 J. D. Ferguson, E. R. Smith, A. W. Weimer and S. M. George, *J. Electrochem. Soc.*, 2004, **151**, G528–G535.
18 S. Tanaka, N. Nishiyama, Y. Oku, Y. Egashira and K. Ueyama, *J. Am. Chem. Soc.*, 2004, **126**, 4854–4858.
19 G. Carturan, R. Dal Toso, S. Boninsegna and R. Dal Monte, *J. Mater. Chem.*, 2004, **14**, 2087–2098.
20 N. Nishiyama, S. Tanaka, Y. Egashira, Y. Oku and K. Ueyama, *Chem. Mater.*, 2002, **14**, 4229–4234.
21 W. Stober, A. Fink and E. Bohn, *J. Colloid Interface Sci.*, 1968, **26**, 62–69.

This journal is © The Royal Society of Chemistry 2010

22 P. Jiang, J. F. Bertone, K. S. Hwang and V. L. Colvin, *Chem. Mater.*, 1999, **11**, 2132–2140.
23 W. C. Oliver and G. M. Pharr, *J. Mater. Res.*, 1992, **7**, 1564–1583.
24 C. J. Brinker and G. W. Scherer, *Sol–Gel Science: The Physics and Chemistry of Sol–Gel Processing*., Academic, 1990.
25 A. Blanco, E. Chomski, S. Grabtchak, M. Ibisate, S. John, S. W. Leonard, C. Lopez, F. Meseguer, H. Miguez, J. P. Mondia, G. A. Ozin, O. Toader and H. M. van Driel, *Nature*, 2000, **405**, 437–440.
26 A. Rugge, J. S. Becker, R. G. Gordon and S. H. Tolbert, *Nano Lett.*, 2003, **3**, 1293–1297.
27 J. S. King, D. Heineman, E. Graungnard and C. J. Summers, *Appl. Surf. Sci.*, 2005, **244**, 511–516.
28 M. Scharrer, X. Wu, A. Yamilov, H. Cao and R. P. H. Chang, *Appl. Phys. Lett.*, 2005, **86**, 151113–151115.
29 M. Born and E. Wolf, *Principles of Optics*, Cambridge University Press, Cambridge, UK, 1997.
30 D. Alkan, in *Encyclopedia of Surface and Colloid Science*, Taylor and Francis, 2006, pp. 5608–5620.
31 L. J. Gibson and M. F. Ashby, *Cellular Solids*, Cambridge University Press, Cambridge, UK, 1997.
32 J. C. Wang, *J. Mater. Sci.*, 1984, **19**, 801–808.
33 N. D. Hoivik, J. W. Elam, R. J. Linderman, V. M. Bright, S. M. George and Y. C. Lee, *Sens. Actuators, A*, 2003, **103**, 100–108.
34 B. Hatton, L, Mishchenko, S. Davis, K. H. Sandhage and J. Aizenberg, *Proc. Natl. Acad. Sci U.S.A.*, DOI: 10.1073/pnas.10000954107.